Transactions on Modelling and Simulation vol 21, © 1999 WIT Press, www.witpress.com, ISSN 1743-355X

Modelling impact forces in elastomers

S. Goyal,[1] R. Larson,[2] C. Aloisio[3]
[1]*Lucent Technologies Bell Laboratories, 600 Mountain Avenue, Rm. 1B-212, Murray Hill, NJ 07974, USA*
EMail: goyal@lucent.com
[2]*Department of Chemical Engineering, University of Michigan, Ann Arbor, MI 53214, USA*
EMail: rlarson@engin.umich.edu
[3]*Lucent Technologies Bell Laboratories, 2000 Northeast Expy, Rm. 2H37, Norcross, GA 30071, USA*
EMail: cjaloisio@bell-labs.com

Abstract

We measure the impact forces and deflections resulting from drop tests of a mass with a flat impact surface onto flat pads of various elastomeric materials, and show that the forces can be predicted quantitatively with no adjustable parameters by using a theory whose only inputs are the linear viscoelastic characteristics of the material, measured in small-amplitude oscillatory deformations. The theory, which models the elastomer as a nonlinear neo-Hookean material, is accurate for several elastomeric solids including polyurethanes, polynorbornene, and poly-vinyl-chlorides (PVCs), over a wide range of impact velocities, masses, temperatures and pad thicknesses. The application in mind is the rational design of elastomeric components in impact-tolerant portable electronic equipment.

1 Introduction

In optimizing the impact-tolerance of a portable electronic product, like a notebook computer, cellular phone, etc., its designer faces two challenges:

(1) Predicting impact-induced loads, and,

(2) Devising strategies for controlling impact loads within stringent constraints that require small size, light weight, low cost and mass-manufacturability.

Goyal et al.[4, 5, 6] have shown that the use of highly dissipative viscoelastic materials in shock-absorbing components like suspensions, grommets, gaskets, and plastic housings is effective in improving the drop-tolerance of portable products.

This paper addresses the issue of predicting forces that would occur in impacts mediated through elastomers. In general the factors that need to be modeled include the viscoelasticity of the rubber, the shape and size of the rubber component and of the impacting surfaces, friction at the interfaces, bulk compression - if any, and the shock waves that are launched into the material due to impact. In an earlier paper (Larson et al.[8]), we showed that a simple constitutive equation for a neo-Hookean rubber could be used to give accurate predictions of impact forces in ideal drop tests of flat objects on thick flat pads of a polyurethane elastomer (called 'Sorbothane') as measured with a commercial drop tester. That work demonstrated the possibility of using simple and easily obtained linear viscoelastic properties of such an elastomer to predict impact forces in 'idealized impacts'. Several further steps are required, however, before the vision of optimal design of elastomeric parts using analytical methods can be realized.

First we must show that the method predicts impact forces equally well with other elastomers, as it does with Sorbothane. The method must then be extended to 'nonideal impacts', such as impacts involving thin pads or surfaces that are not flat - like the corners and edges of a product. The final goal would be incorporation into new or existing drop-test-simulation software. However the predictive model can be used even before this final step - to get cushioning efficiency curves, for instance - as will be discussed.

In this paper, we show that our predictive model for impact forces is accurate for solid elastomeric materials in general, by studying several other commercial-materials that are recommended for shock-protection. We also demonstrate that the model can give correct results for peak impact force, duration, and maximum pad deflection, even for impacts involving very thin pads of these elastomers - as thin as those that are likely to be used in applications - without addition of any arbitrary fitting parameters.

2 Materials studied

As discussed in Larson et al.[8], high energy dissipation during impact (or shock-absorbtion) at a given temperature occurs in elastomers that are in their 'viscoelastic transition zones' between rubbery and glassy behavior at that temperature, for frequencies characteristic of typical impacts, around $10^2 - 10^4 s^{-1}$. Equivalently, a high rate of viscous dissipation can most readily be achieved in a material whose glass transition temperature T_g is a few tens of degrees Celsius below the temperature at which impact occurs.(The other significant factor in determining the usefulness of an elastomer in shock-protection applications is its dynamic modulus.) The amount of viscous damping is controlled by the extent of the

transition zone. The sharper the transition zone, the higher the viscous dissipation during impact. However, a sharp transition zone also implies that mechanical properties of the polymer are very sensitive to temperature (and frequency) changes. So, good impact-absorbing performance over a wider effective temperature range frequently comes at the expense of lower dissipativeness.

There are several methods of engineering polymers to have the above properties. For instance, in the case of Sorbothane 70 (studied by Larson et al.[8]), a single-phase material is found with $T_g = -59.5°C$, and the crosslink density is kept low to yield a transition zone in the $10^2 - 10^4$ s^{-1} frequency window at room temperature. In this paper, we present results for three additional elastomers that represent other methods for achieving high damping at room temperature and whose compositions differ significantly from Sorbothane. The materials are:

(1) 'Wingfoot XL', a material based on the amorphous polymer polynorbornene, manufactured by Goodyear Shoe Products, Hudson, NH. The composition of Wingfoot XL (Pilkington et al.[9, 10]), by weight, is roughly 10 parts polynorbornene, 14 parts paraffinic oils, and 4 parts resin. The resin is incompatible with polynorbornene, forming an eutectic mixture, and acts like a filler to modify the modulus. Polynorbornene is by itself a glassy polymer, $T_g \approx 43°C$, but in powdery form it has tremendous affinity for paraffinic oils and can absorb and retain a large amount of them due to its cage-like molecular structure. The paraffinic oils act as plasticizers to lower its glass transition temperature. It is this interaction between the paraffinic solvent and polynorbornene that gives Wingfoot XL a highly dissipative character at room temperature. We determined $T_g \approx -3.5°C$ for Wingfoot XL.

(2) E.A.R. C-1002, a PVC material, made by E.A.R. Speciality Composites, Indianapolis, IN. E.A.R. C-1002 is a plasticized PVC (E.A.R.[1]). The plasticizer is a medium-to-high molecular weight oil with a low migration rate. $T_g \approx -5.2°C$ was determined for E.A.R. C-1002.

(3) 'Impactek', a material marketed by Frelonic Corporation, Salem, MA. We do not know the composition of Impactek; its T_g was determined to be $15.2°C$.

High damping materials that encompass other strategies, like blending different polymers (e.g., block copolymers) and foaming, will be discussed in a subsequent paper.

3 Experimental results

Two basic kinds of experiments were performed on each material selected for our study: (*a*) measurement of the linear viscoelastic spectrum (also known as the 'master curve', or the 'reduced frequency nomogram'), and, (*b*) measurement of forces and deflections in drop tests involving pads of the material.

Table 1. Viscoelastic Shift Factors for Reference $T = 20°C$

Temperature	$\log_{10} a_T$		
$°C$	Wingfoot XL	E.A.R. C-1002	Impactek
−80	—	14.3	11.18
−70	—	13.5	10.98
−60	—	13	10.58
−50	8.96	12	10.18
−40	8.56	10.2	9.68
−30	8.16	8	9.08
−20	6.96	6	7.37
−9	5.26	4	5.47
0	3.16	2.4	3.25
10	1.46	0.5	1.5
20	0	0	0
30	−1.11	−1	−1.4
40	−1.94	−1.8	−2.61
50	−2.91	−3.4	−3.42
61	—	—	−4.22
70	—	—	−4.62
80	—	—	−5.02

3.1 Viscoelastic measurements

Viscoelastic properties of the elastomers used in our study were characterized through small-amplitude oscillatory tests using the Rheometrics Solids Analyzer (RSA) in tension-tension mode, as described in Larson et al.[8]. At each of the temperatures in Table 1, the tensile storage modulus E' and the tensile loss modulus E'' were measured at frequencies ω ranging from $0.1 - 100$ rad/s. Because of the equivalent effect of frequency and temperature (e.g. Ferry[2]), in the absence of any structural or chemical changes during the test, the moduli at each individual temperature can be shifted along the log frequency axis to form a master curve at the reference temperature of $20°C$. The shift factors a_T for the three elastomers at each temperature are tabulated in Table 1. As an example, the master curve for Wingfoot XL is shown in Fig. 1.

The shear storage and loss moduli, G' and G'', are related to the corresponding tensile moduli by

$$G' = \frac{E'}{1+\nu} \quad ; \qquad G'' = \frac{E''}{1+\nu} \tag{1}$$

In the low-frequency, low-modulus, rubbery zone, Poisson's ration $\nu \approx 0.5$, and eqn. (1) reduces to $G' = E'/3$, and $G'' = E''/3$. These relationships are used for all of the data in Fig. 1. Although these relationships are not exact in the high-frequency, high-modulus, glassy zone, data in this region are not particularly important to the impact properties of the material, at least at or above room

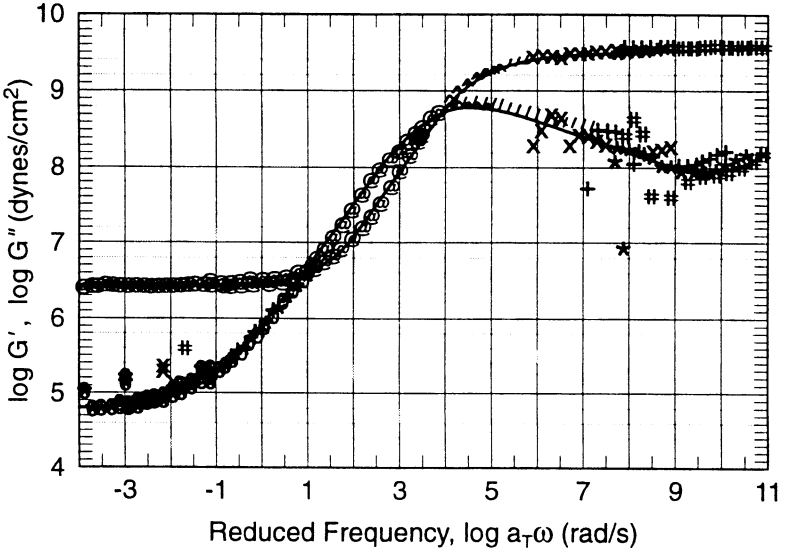

Figure 1: Master Curve of G' and G'' versus reduced frequency $\log(a_T\omega)$ for Wingfoot XL, at a reference temp. of $20°C$. It is the superposed curve produced by shifting 'dynamic modulus isotherms', obtained at each temp. listed in Table 1, along the reduced frequency axis by an amount $\log a_T$ (also given in Table 1).

temperature.

The shift factors $\log a_T$ obtained during the construction of the master curve for a given material can be plotted versus temperature, as shown in Fig. 2 for Wingfoot XL and Sorbothane 70. Using a so-called 'WLF fit' to the data of the above plot, a glass transition temperature can be determined for the material (e.g. Ferry[2]). Observe in Fig. 2 that near room temperature, the slope of the plot of the shift factor versus temperature is steeper for Wingfoot XL than that for Sorbothane 70, implying that the former is more temperature sensitive. Thus, the ideal impact-absorbing properties of Wingfoot XL erode quickly with temperature. On the other hand the lower T_g of Sorbothane 70, coupled with the lower temperature sensivity of its shift factor, make it a better impact-absorber than Wingfoot XL at low temperatures.

Hence, as mentioned earlier, optimal design of a viscoelastic elastomer for shock-protection will generally involve a trade-off between its dissipative properties and its temperature sensitivity.

3.2 Discrete fits to dynamic moduli

The viscoelastic response, or the evolution of stress, in the elastomer during impact can be modelled as arising from a spectrum of exponentially decaying relaxation

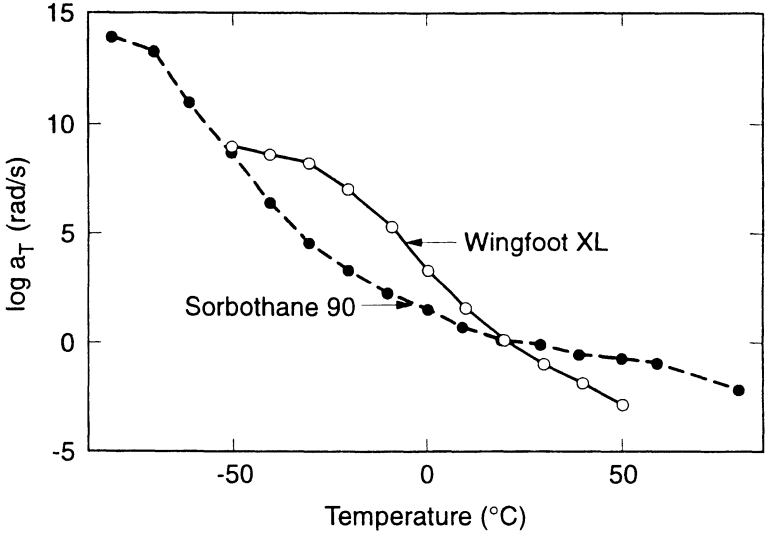

Figure 2: Plot of the temperature dependences of the shift factors used to obtain the master curves for Wingfoot XL and Sorbothane 70 (from Larson et al.[8]).

phenomenon. Hence the frequency dependent storage and loss moduli $G'(\omega)$ and $G''(\omega)$ can, in general, be fitted to expressions involving spectrum of relaxation times τ_i and strengths G_i:

$$G'(\omega) = \sum_i \frac{G_i \omega^2 \tau_i^2}{1 + \omega^2 \tau_i^2} \; ; \qquad G''(\omega) = \sum_i \frac{G_i \omega \tau_i}{1 + \omega^2 \tau_i^2} \tag{2}$$

For purposes of impact modelling the G' and G'' curves need only be fit out to the highest frequencies that influence the impact forces; typically, fits out to a frequency of around 10^5 s^{-1} are adequate. Note that the highest frequency for which a fit is obtainable is set by the reciprocal of the shortest relaxation time τ_i in the assumed spectrum. If the fit is extended to include frequencies higher than 10^5 s^{-1}, relaxation times that are shorter than necessary are brought into the relaxation spectrum, and this greatly increases the computation required for simulation of the drop tests. (The time step for explicit integration in our simulation has to be smaller than the smallest relaxation time in the spectrum to preserve numerical stability.)

Hence, it is desirable to exclude from the set of relaxation times those values that are too short to influence the impact forces. Such very fast modes are almost completely relaxed out on the time scale of the impact - typically a few milliseconds (ms) - and contribute only a small viscous-like dissipative stress, which can be characterized by a viscosity η. Therefore, we choose a set of $12 - 16$ well spaced

relaxation times spanning the time range of interest, and adjust values of the corresponding G_i's to obtain a fit of eqn. (2) to G' and G'' for each material. In the simulations to be described below, the viscosity η is shifted along with the relaxation spectrum to account for changes in temperature; that is, η and the τ_i's are multiplied by the same temperature-dependent shift factor a_T. Since changes in temperature shift the G' and G'' curves along the frequency axis, the number of 'relaxation modes' (pairs of G_i and τ_i values) that must be included in the spectrum depends on the test temperature. Also, for fast impacts produced by drops onto thin pads, more modes must be included to obtain accurate predictions of the high-frequency response.

Table 2. Viscoelastic Constants at $20°C$

i	τ_i(s)	Wingfoot XL		E.A.R. C-1002	Impactek
		G_i(Pa)	η(Poise)	G_i(Pa)	G_i(Pa)
1	10000	0.25e+06		1.5e+06	0.80e06
2	1000	0.004e+06		0.015e06	0.008e06
3	100	0.004e+06		0.05e06	0.12e06
4	30	0.004e+06		0.015e06	0.08e06
5	10	0.010e+06		0.10e06	0.14e06
6	3	0.015e+06		0.15e06	0.20e06
7	1	0.040e+06		0.2e06	0.25e06
8	0.3	0.050e+06		0.4e06	0.55e06
9	0.1	0.06e+06		0.5e06	0.90e06
10	0.03	0.20e+06		0.7e06	0.90e06
11	0.01	0.6e+06		1.2e06	1.05e06
12	0.003	1.5e+06		2.0e06	2.0e06
13	0.001	1.1e+07	5000	0.8e07	3.0e07
14	0.0001	8.0e+07	500	2.0e07	9.9e07
15	0.00001	1.0e+08	20	0.7e08	2.0e08
16	0.000001	5.0e+07	2		

Table 2 gives the 'best-fit' values of the G_i's corresponding to a set of specified τ_i's for the three elastomers. Additionally, for Wingfoot XL, several different viscosities are presented. Each viscosity corresponds to the cut-off relaxation time listed in the same row of Table 2. For instance, $\eta = 5000$ Poise represents the viscosity due to all the relaxation modes that are faster than 0.001 s. For E.A.R. C-1002 and Impactek, the viscosities for relaxation modes faster than 0.00001 s are 50 Poise and 100 Poise respectively.

3.3 Drop tests

Drop-test data for the rubber pads were collected using Dynatup impact testing machine Model 8250, as explained in Larson et al.[8]. The cylindrical elastomeric pads ranged in diameter from $25.4 - 38.1$ mm, and $3.05 - 25.4$ mm in thickness.

The impacting mass was around 1.81 kg at room temperature and around 2.27 kg at lower or higher temperatures. Impact data were collected at room temperature (which varied from run to run from 20°C to 26°C), at 5°C, and at 40°C. The simulations were carried out using the viscoelastic spectrum shifted to the temperature at which the run was made.

4 Impact model

The equations for a simple uniaxial impact are given by Newton's second law, $F = m\ddot{x}$, and by relating the impact force F and the uniaxial stress σ in the material:

$$m\ddot{x}(t) = A(t)\sigma(t) \tag{3}$$

In eqn. (3), m is the impacting mass, $A(t)$ is the instantaneous area of impact, and $\ddot{x}(t)$ the instantaneous acceleration of the impacting mass. Assuming volume conservation, $A(t) = A_0 x_0/x(t)$, where A_0 and x_0 are the initial area and thickness of the pad respectively.

The uniaxial viscoelastic stress σ_{ve} can be obtained from a model constitutive equation for an ideal Hookean incompressible viscoelastic material (e.g. Treloar[11]):

$$\sigma_{ve} = \int_{-\infty}^{t} m(t-t')[\lambda(t,t') - \lambda^{-2}(t,t')]dt' \tag{4}$$

Here $\lambda(t,t') \equiv x(t')/x(t)$ is the deformation produced during the time interval between time t' and time t. Equation (4) assumes that the deformation is a purely uniaxial one, which implies that the elastomer does not adhere strongly to the contacting surface.

The function $m(t-t')$ contains the material's viscoelastic properties and is derived from the time-dependent linear modulus $G(t-t')$ using

$$m(t-t') \equiv \frac{dG(t-t')}{dt'} \tag{5}$$

The linear modulus $G(t-t')$, in turn, can be obtained from the G_i's and τ_i's extracted from dynamic oscillatory data for each material, as discussed in section 3.2. Then, $G(t-t')$ is given by,

$$G(t-t') = \sum_i G_i e^{-(t-t')/\tau_i} \tag{6}$$

To the viscoelastic stress σ_{ve} is added a viscous-flow stress $\sigma_v = -3\eta\dot{x}/x$ which represents contributions from modes faster than those included in the spectrum. Hence,

$$\sigma = \sigma_{ve} - 3\eta\dot{x}/x \tag{7}$$

Here, $-\dot{x}/x$ is the rate of strain in a uniaxial compression and the factor of 3 enters because of Trouton's ratio (e.g. Larson[7]) for volume-conserving deformations.

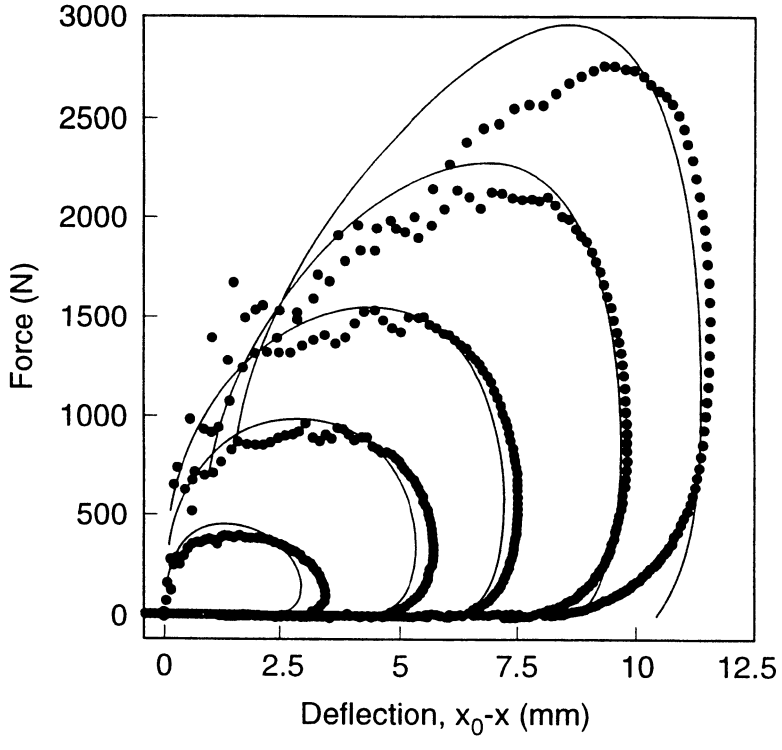

Figure 3: Force as a function of deflection, for a sample of Wingfoot XL with an initial diameter of 24.6 mm and thickness 25.4 mm, impacted by a mass of 1.81 kg, at 25 $\pm$ 1°C. Impact velocities are $v_0 = 1.04, 2.11, 3.08, 4.11,$ and 4.93 m/s. In this and the following plots of impact force, the symbols represent experimental data and the lines are predictions of the theoretical model.

5 Simulation results

Using eqns. (3)-(7), and the viscoelastic constants from Table 2, we can now predict the forces generated during impact by solving the momentum-balance equation, with no adjustable parameters. Figure 3 shows the measured and predicted impact force as a function of deflection for Wingfoot XL at room temperature, 25°C. Excellent agreement is obtained between measured and predicted forces, similar to the agreement found with a pad of Sorbothane 70 (e.g. Larson et al.[8]).

Figure 4 shows the impact force versus deflection for Wingfoot XL at 5°C and 40°C respectively. Note the enormous difference in impact force and deflection produced by these temperature changes, illustrating the very high temperature sensitivity of the viscoelastic properties of Wingfoot XL near room temperature.

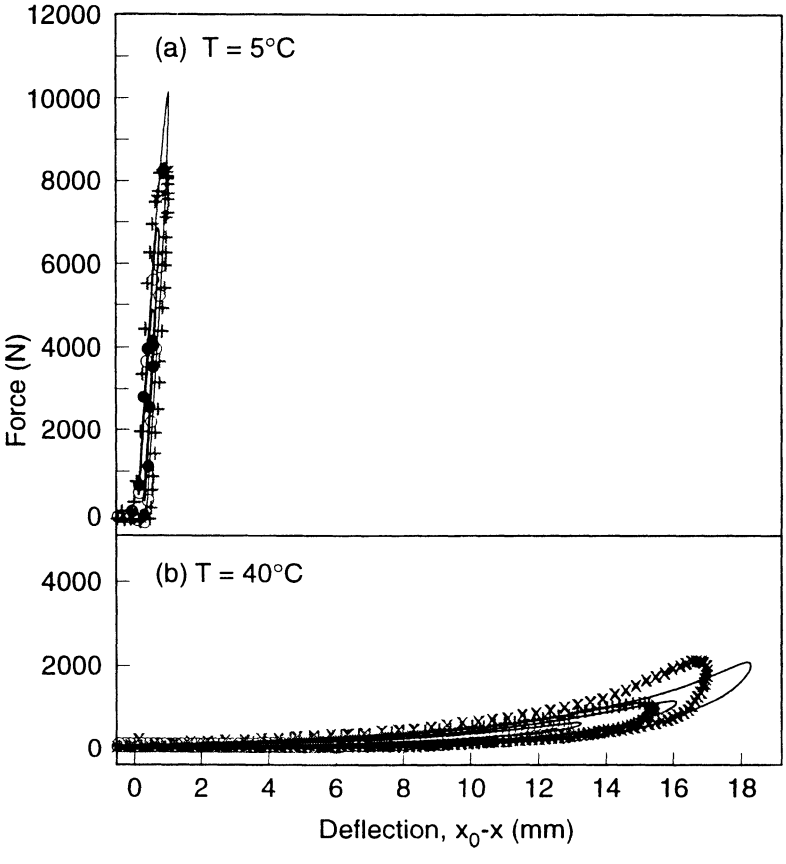

Figure 4: Force as a function of deflection, for a sample of Wingfoot XL with initial diameter 24.6 mm and thickness of 25.4 mm, impacted by a mass of 2.27 kg, at *(a)* $T = 5 \pm 1°C$, and *(b)* $40 \pm 1°C$. The impact velocities are *(a)* $v_0 = 1.04, 1.48$, and 2.16 m/s, and *(b)* $v_0 = 1.12, 1.66, 2.34$, and 3.05 m/s.

We now consider the effect of pad size on impact characteristics. Figures 3 and 5 show that for Wingfoot XL, good agreement with the model is also obtained when the pad diameter is varied in the range $25.4-38.1$ mm. To determine whether the model can describe impacts involving thin pads, we tested Wingfoot XL pads with thicknesses down to 3.05 mm. Figure 6 shows that the most important gross characteristics of an impact, namely the peak force and the maximum deflection, are fairly accurately predicted by the model, even for the thinnest pad. Note, however that as the pad becomes thinner, the measured force appears to become noisier; the noise is especially prominent in the 3.05 mm thick pad. The apparent

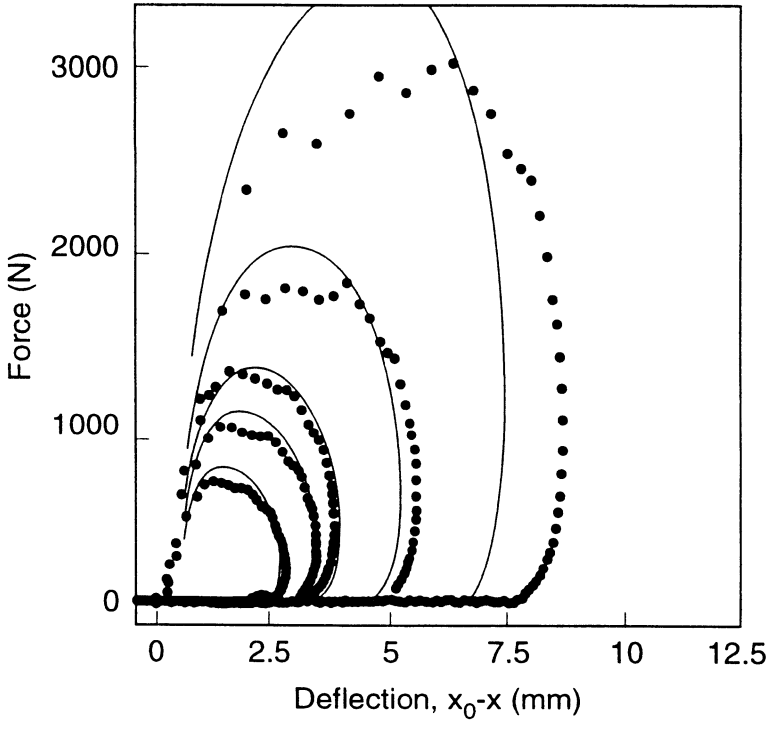

Figure 5: Force as a function of deflection, for a sample of Wingfoot XL with initial diameter 37.3 mm and thickness 25.4 mm, impacted by a mass of 1.81 kg, at T = 26 ± 1°C. The impact velocities are v_0 = 1.26, 1.75, 2.11, 3.08, and 4.94 m/s.

noise in these thin-pad data is produced by a fairly regular oscillation in force as a function of time; see Fig. 7. The period of the oscillation is around 0.35 – 0.25 ms, decreasing somewhat as the impact velocity increases. These oscillations are not predicted by the model.

The existence of the oscillations, and their increasing severity with decreasing pad thickness, suggest that they are caused by a viscoelastic deformation wave that is launched into the material on impact. Since the elastomer is viscoelastic, and not purely elastic, any such wave will disperse or damp out over time. For thin enough bodies, however, the time required for the wave to propagate through the pad and to be reflected back to the point where the force is measured might become comparable to the time required to dissipate the wave. In such a case, an oscillation, or 'ringing' of the force transducer would occur, such as that shown in Fig. 7. For an ideal elastic body, the speed of a deformation wave moving through the pad is roughly $\sqrt{G/\rho}$, where G is the elastic modulus and ρ is the material density. At the frequency of the impact, the modulus of Wingfoot XL is roughly

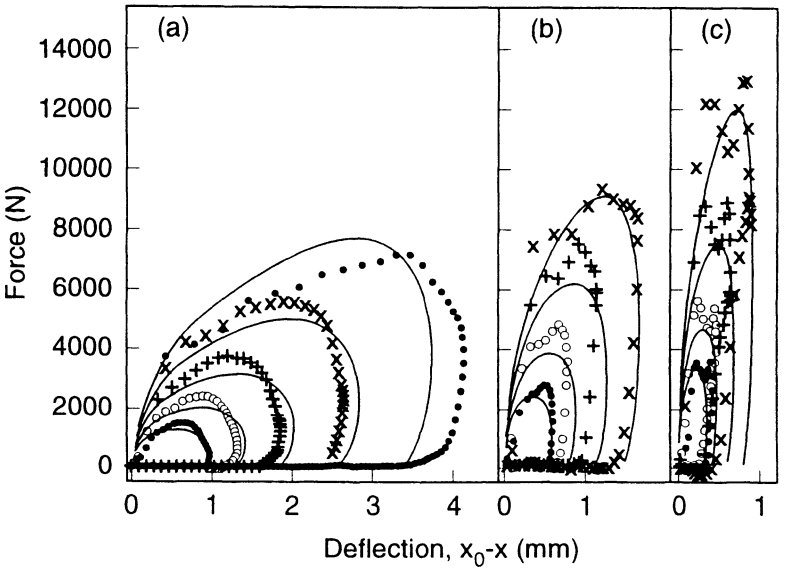

Figure 6: Force as a function of deflection for samples of Wingfoot XL of varying thickness, impacted by a mass of 1.81 kg. *(a)* $x_0 = 12.0$ mm, $D_0 = 26.7$ mm, T = 22±1°C, and $v_0 = 1.06, 1.60, 2.38, 3.51$, and 4.94 m/s. *(b)* $x_0 = 6.25$ mm, $D_0 = 27.4$ mm, T = 22 ± 1°C, and $v_0 = 1.10, 1.73, 2.62$, and 3.62 m/s. *(c)* $x_0 = 3.05$ mm, $D_0 = 27.4$ mm, T = 23±1°C, and $v_0 = 1.03, 1.41, 2.12$, and 3.05 m/s.

10^7 N/m^2, which would yield a wave speed of around 10^2 m/s, if the material were purely elastic. Propagation of a wave of this speed through a pad 3 mm thick, and reflection of that wave back to the impacting surface would therefore require around 0.06 ms, which is about three times smaller than the observed oscillation period. Of course, our material is far from being purely elastic, and an accurate estimation of the wave speed and its rate of dissipation would require a complex analysis of a nonuniform time-dependent deformation of the elastomer under the given impact conditions.

Whatever the source of the oscillation is, the important point for our purposes is that it does not greatly affect the peak force, maximum deflection, or impact duration, at least for pads no thinner than 3 mm thick. Thus, our simple analysis, which cannot predict such oscillations, can still be used to predict the important gross features of the impact, even for fairly thin pads.

Drop tests were also performed for E.A.R. C-1002 and Impactek over a range of drop heights similar to that used for Wingfoot XL. Using the constants shown in Table 2, the impact predictions for these materials are in good-to-excellent agreement with the experimental results; see Figs. 8 and 9.

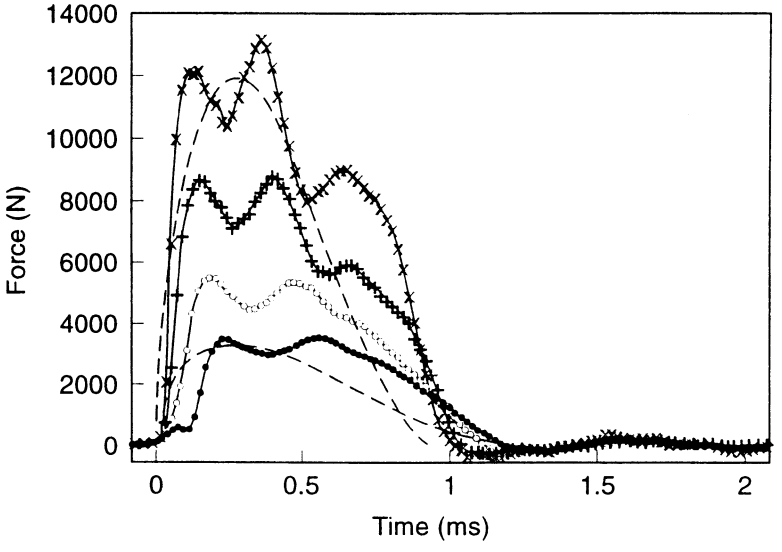

Figure 7: The data in Fig. 6(c) for a 3.05 mm thick pad of Wingfoot XL are replotted as force versus time. The solid lines are guides to the eye; the dashed lines are the model predictions for the lowest and highest velocity impacts.

6 Cushioning efficiency - 'J curves'

To facilitate material selection, and the design of rubbery components, suppliers of impact-absorbing materials frequently summarize impact performance data in the form of an experimentally determined curve, called the 'J curve'. The J curve is a plot of dimensionless peak force $J = F_{max}x_0/Wh$, against impact energy density $U = Wh/x_0A_0$, where F_{max} is the maximum force generated during impact. An ideal impact-absorbing material, that generates the lowest peak force for given impact conditions, is one that produces constant force with deformation and allows its entire thickness x_0 to be used as 'stopping distance'. The minimum impact force thus produced can be shown to equal Wh/x_0. Hence, the value of J corresponds to the actual peak force relative to the lowest possible peak force. Since no impact absorbing material can behave in the theoretically ideal way described above, J values always exceed unity.

The motivation for plotting J versus U comes from a dimensional analysis originally described by Woolam[12]; the equation of motion (3) can be rewritten as,

$$2(\frac{x_0}{v_0})^2\ddot{X} = \frac{1}{U}\frac{1}{X}\sigma(X(t)) \tag{8}$$

where $X \equiv x/x_0$ is the dimensionless instantaneous pad thickness, which is related to the instantaneous strain by $\lambda = 1/X$. Equation (8) implies that $X(t)$, and hence

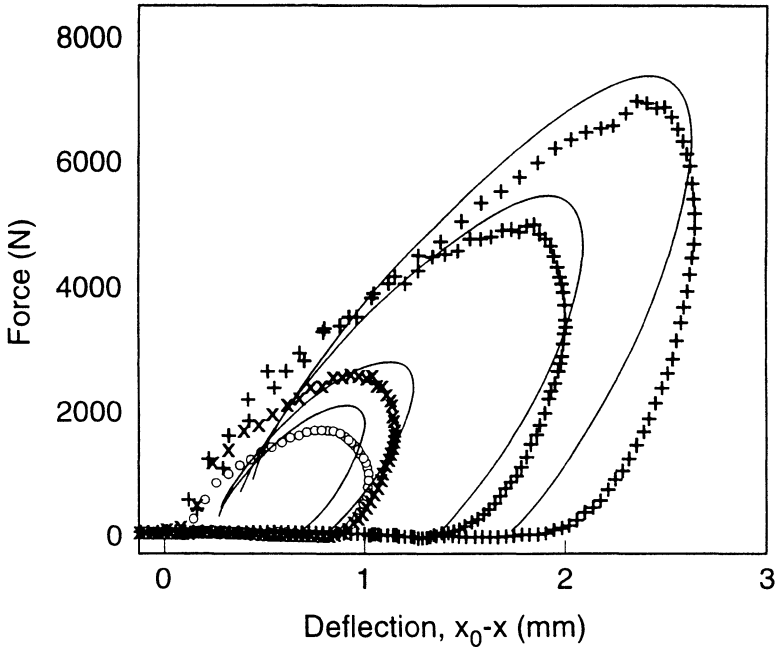

Figure 8: Force as a function of deflection for a sample of E.A.R. C-1002 with an initial diameter of 32.4 mm, and thickness of 12.5 mm, impacted by a mass of 1.81 kg, at $T = 20 \pm 1°C$. Impact velocities are $v_0 = 1.06, 1.41, 2.61,$ and 3.42m/s.

peak force, depend on U and v_0/x_0.

For purely elastic materials, the peak force would be a function of U only and values of J for a single material under varying drop conditions - weight, height, and thickness and area of pad - will fall on a single curve. For time-dependent materials, however, the J curve will depend both on U and v_0/x_0. Figure 10, for example, shows the J curves calculated using our impact theory for Wingfoot XL under conditions in which the drop mass is varied at fixed impact velocity (that is, only U is changing), and under conditions in which the impact velocity is varied and the mass kept fixed (so both U and v_0/x_0 are changing). In both cases, the thickness and area of the pad are held fixed. Note that substantially different curves are obtained in the two cases; their J minima are spaced more than an order of magnitude apart on the U-axis. A whole family of J curves of the type shown in Fig. 10 can be generated for Wingfoot XL by varying drop velocity at each of a series of masses, or, conversely, by varying drop mass at a series of drop velocities.

Despite the dependence of the J curve on drop conditions, its usefulness

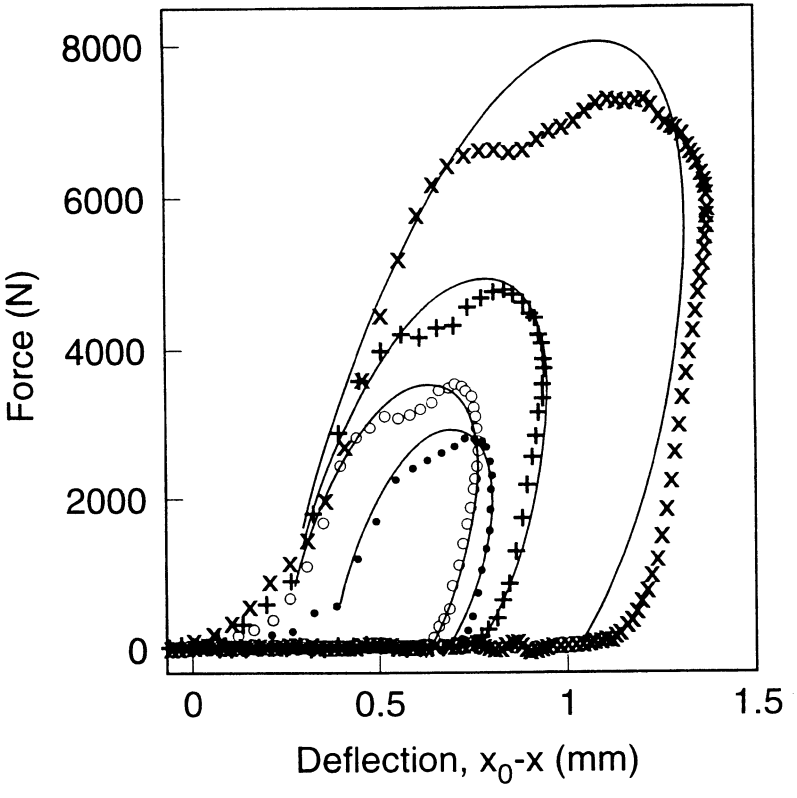

Figure 9: Force as a function of deflection for a sample of Impactek solid with an initial diameter of 25.1 mm, and thickness of 9.86 mm, impacted by a mass of 1.81 kg, at $T = 20 \pm 1°C$. Impact velocities are $v_0 = 1.01, 1.23, 1.69$, and 2.66m/s.

as an engineering tool stems from the existence of a minimum in the J curve, suggesting the existence of a 'maximum cushioning efficiency'. The location of the minimum along the U-axis characterizes the drop conditions for which the material is especially well suited for optimal use of its cushioning ability. Given the wide separation in 'fixed-velocity' and 'fixed-mass' J curves for Wingfoot XL, as shown in Fig. 10, it may be prudent to use the fixed-mass J curve for designing elastomeric parts for a given portable product. This is because the effective mass of the product (e.g. Goyal et al.[3]) in accidental drops will vary much less than the impact velocity, which depends on the height from which the object is dropped.

7 Conclusions and future directions

We have shown that a simple uniaxial impact model for elastomers, proposed by Larson et al.[8], predicts forces and deflections as well for Wingfoot XL,

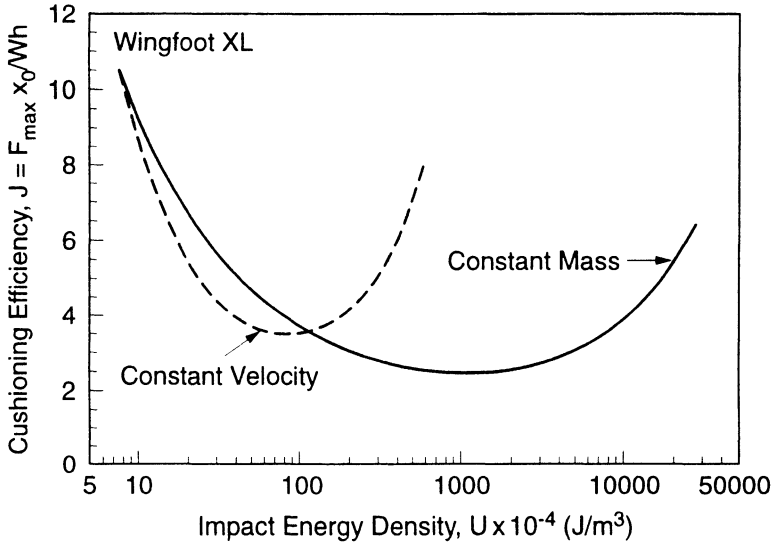

Figure 10: Cushioning efficiency 'J' curves calculated for a pad of diameter 24.6 mm and height 25.4 mm of Wingfoot XL. The constant mass curve is for an impacting mass of 1.81 kg and the constant velocity curve is for an impact velocity of 1.04 m/s.

Impactek, and E.A.R. C-1002, as it does for Sorbothane 70 in drop tests using flat pads and flat impact surfaces. This shows that the linear viscoelastic spectrum in general adequately characterizes the impact properties of such commercially available rubbery materials that are recommended for use in shock-protection of products. In addition, comparisons of the impact properties of these materials can now be made, and the differences between them can be traced to differences in their relaxation spectra - a fundamental and engineerable property.

We have also shown that the important characteristics of the impact, namely its maximum force, pad deflection, and impact duration, can be predicted even for pads of Wingfoot XL as thin as 3 mm, even though oscillations present in the thin-pad data (probably due to viscoelastic-wave propagation) are not predicted. The ability to predict impact forces in very thin pads is important in light-weight designs for portable electronic products, in which the mass and size of elastomer used for shock-protection is reduced to a bare minimum.

The next steps in our research program are to predict impact forces for foamed materials, which are popular for impact protection, and to develop general material design principles that allow choice of the optimal material - one that minimizes the peak impact force - for a given set of impact conditions including temperature.

References

[1] E.A.R. Speciality Composites, *Technical Data Sheet TDS-19*, Indianapolis, IN, 1996.

[2] Ferry, J.D., *Viscoelastic Properties of Polymers*, Third Edition, John Wiley & Sons, New York, 1980.

[3] Goyal, S., Pinson, E.N. & Sinden, F.W., Simulation of Dynamics of Interacting Rigid Bodies Including Friction II: Software System Design and Implementation, *Engineering With Computers*, **10**(3), pp. 175-195, 1994.

[4] Goyal, S., Papadopoulos, J.M. & Sullivan, P.A., Shock Protection of Portable Electronic Products: Shock Response Spectrum, Damage Boundary Approach, and Beyond, *Shock and Vibration*, **4**(3), pp. 169-191, 1997.

[5] Goyal, S., Papadopoulos, J.M. & Sullivan, P.A., The Dynamics of Clattering I: Equation of Motion and Examples, *Journal of Dynamical Systems, Measurement, And Control*, **120**(1), pp. 83-93, 1998.

[6] Goyal, S., Papadopoulos, J.M. & Sullivan, P.A., The Dynamics of Clattering II: Global Results and Shock Protection, *Journal of Dynamical Systems, Measurement, And Control*, **120**(1), pp. 94-102, 1998.

[7] Larson, R.G., *Constitutive Equations for Polymer Melts and Solutions*, Butterworths, Boston, 1988.

[8] Larson, R.G., Goyal, S. & Aloisio, C.J., A Predictive Model for Impact Response of Viscoelastic Polymer in Drop Tests, *Rheologica Acta*, **35**, pp. 252-264, 1996.

[9] Pilkington, M., Creasey, J. & Becken, R., Energy Absorbing Rubber Composition, *United States Patent Number 4504604*, March 12, 1985.

[10] Pilkington, M., *personal communication*, Goodyear Tire Company, Akron, OH, May 15, 1995.

[11] Treloar, L.R.G., *The Physics of Rubber Elasticity*, Third Edition, Clarendon Press, Oxford, UK, 1975.

[12] Woolam, W.E., A Study of the dynamics of low energy cushioning materials using scale models, *J. Cellular Plastics*, **4**, pp. 79-83, 1968.